Influence of surface topography on bacterial adhesion: A review (Review)

Songze Wu, Botao Zhang, Yi Liu, Xinkun Suo, and Hua Li

Citation: Biointerphases **13**, 060801 (2018); doi: 10.1116/1.5054057
View online: https://doi.org/10.1116/1.5054057
View Table of Contents: https://avs.scitation.org/toc/bip/13/6
Published by the American Vacuum Society

Influence of surface topography on bacterial adhesion: A review (Review)

Songze Wu,[1,2,a)] Botao Zhang,[1,b)] Yi Liu,[1,c)] Xinkun Suo,[1,d)] and Hua Li[1,e)]
[1]*Key Laboratory of Marine Materials and Related Technologies, Zhejiang Key Laboratory of Marine Materials and Protective Technologies, Ningbo Institute of Materials Technology and Engineering, Chinese Academy of Sciences, Ningbo 315201, China*
[2]*School of Physical Science and Technology, ShanghaiTech University, Shanghai 201210, China*

(Received 29 August 2018; accepted 1 November 2018; published 27 November 2018)

Bacterial adhesion and biofilm formation are ubiquitous undesirable phenomena in the marine industry and the medical industry, usually causing economic losses and serious health problems. Numerous efforts have been made to reduce bacterial adhesion and subsequent biofilm formation, most of which are based on the release of toxic biocides from coatings or substrates. In recent years, surface topography has been found to substantially influence the interaction between bacteria and surfaces. This review summarizes previous work dedicated in searching for the relationship between bacterial adhesion and surface topography in the last eight years, as well as the proposed mechanisms by which surface topographic features interact with bacterial cells. Next, various natural and artificial surfaces with bactericidal surface topography along with their bactericidal mechanisms and efficiency are introduced. Finally, the technologies for constructing antibacterial surfaces are briefly summarized. https://doi.org/10.1116/1.5054057

I. INTRODUCTION

Biological fouling, also referred to as biofouling, is undesirable accumulation and proliferation of microorganisms, plants, or animals on natural or artificial surfaces. Biofouling is a major problem affecting the functional service duration of marine industrial facilities and medical implants (Fig. 1).[1] In the marine industry, for boats, ships, and submarines, biofouling usually brings about sailing resistance, causing higher fuel consumption and increased waste emissions.[2] Biofouling can also inflict substantial damage to coatings and substrates, causing severe corrosion, reducing service duration, and increasing maintenance costs. Furthermore, as ships travel all around the world, so do the adhering creatures.[3] Introduction of invasive species may compromise local ecological balance. In the medical area, pathogenic bacteria such as *Staphylococcus aureus*, *Escherichia coli*, and *Pseudomonas aeruginosa* adhering to medical devices such as catheters and implants can cause serious infections and even death, as well as higher healthcare costs.[4]

Bacterial adhesion is the first step of biofilm formation. Planktonic bacterial cells initially attach to an available surface, then proliferate and secrete extracellular polymeric substances (EPSs), and finally multilayer cells cluster and form biofilms (Fig. 2). Bacterial cells living in biofilms are more resistant to external physical stress, chemical biocides, and antibiotics compared to planktonic cells, making them extremely difficult to be removed.[5] Therefore, inhibiting initial bacterial adhesion is essential for preventing biofilm formation. Altering the surface chemistry is thought to be an effective method to deter bacterial adhesion. Embedding toxic biocides and grafting functional groups are commonly used surface chemistry alteration processes. Numerous efforts have been made to reduce bacterial adhesion via releasing toxic biocides from coatings or substrates.[6–10] However, the release of toxic substances into the environment can cause catastrophic effects on the ecosystem. For example, tributyltin (TBT) self-polishing copolymer paints were widely used in biocide-based antifouling coatings. The biocide TBT is very effective and led to considerable economic benefits. Unfortunately, the use of TBT has been banned due to its adverse effects on a wide variety of marine species. Antibiotics can also be rendered ineffective in the long term owing to the development of resistance by bacterial species.[11,12] Moreover, due to the gradual loss of biocides, the long-term effectiveness of this method remains to be further improved. Another established strategy is grafting functional groups onto surfaces using surface chemical modification methods for killing adhering bacterial cells or changing surface wettability and therefore hindering bacterial adhesion.[13,14] The effectiveness of this strategy is also transient due to the desorption of functional molecules over time and the consequent masking of surface chemistry by adsorbed proteins and exopolysaccharides secreted by bacteria.

In recent years, surface topography has been found to substantially influence the interaction between bacteria and surfaces. Physical alteration of surfaces is believed to be a promising alternative to chemical modification as it provides long-term effectiveness and environmental friendliness.[15] Surface roughness and surface topographical features are the factors that physically affect bacterial adhesion on surfaces and have drawn extensive concern. Antibacterial surfaces can

[a)]Electronic mail: wusongze@nimte.ac.cn
[b)]Electronic mail: zhangbotao@nimte.ac.cn
[c)]Electronic mail: liuyi@nimte.ac.cn
[d)]Author to whom correspondence should be addressed: suoxinkun@nimte.ac.cn
[e)]Electronic mail: lihua@nimte.ac.cn

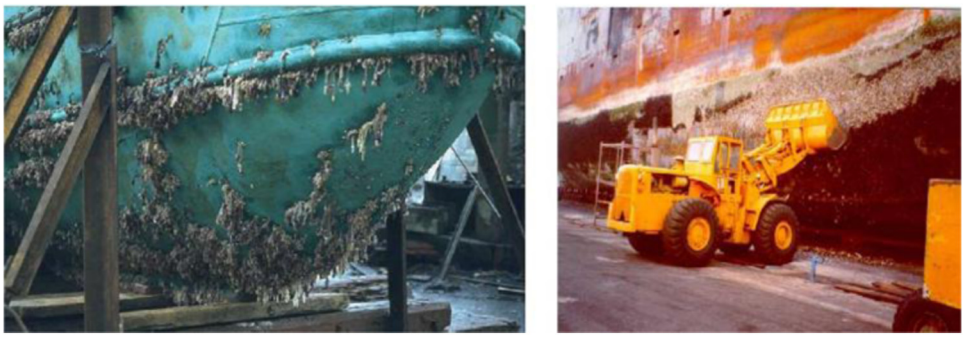

FIG. 1. Examples of marine biofouling. Reprinted from D. M. Yebra *et al.*, Prog. Org. Coat. **50**, 75 (2004). Copyright 2003, Elsevier.

be categorized as antiadhesion surfaces and bactericidal surfaces. Antiadhesion implies preventing bacterial cells from attaching to a surface through unfavorable surface topography.[16] Bactericidal surfaces involve the surfaces with some special structures which can destroy the cell membrane of bacteria and kill them. In this review, we summarized the commonly used antibacterial surfaces and the proposed mechanisms by which surface topographical features deter bacterial adhesion or kill adhering bacterial cells. Furthermore, the commonly used approaches for fabricating antibacterial surfaces are also summarized.

II. ANTIADHESION SURFACE TOPOGRAPHY

Surface properties including surface charge, surface free energy, and surface wettability have been shown to influence bacterial adhesion.[17] For example, a lot of studies focused on the potential use of superhydrophobic surfaces in preventing bacterial adhesion and biofilm formation.[18–21] Nevertheless, the majority of the current studies focused on describing the phenomenon, and they applied different materials and methods. The surface properties mentioned above are often the synergistic results of surface chemical composition and surface topography. This review emphasizes on the physical interaction between bacterial cells and surface topography, and the effect of surface chemistry is therefore neglected.

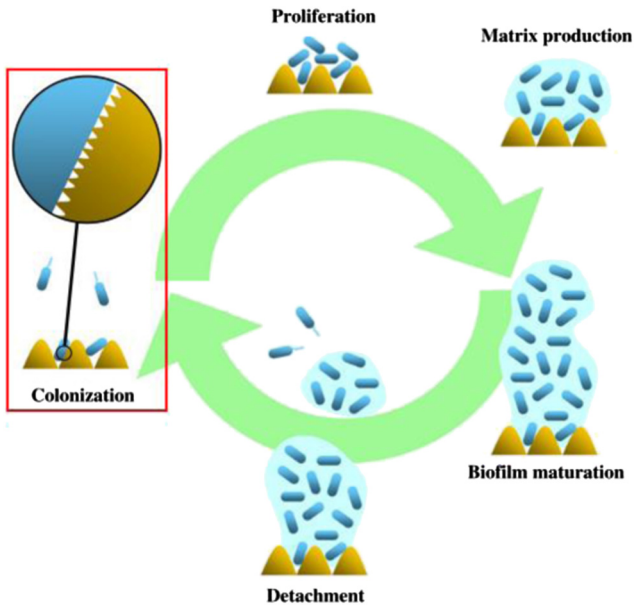

FIG. 2. Life cycle of biofilm formation on a hierarchically rough surface. Reprinted from R. J. Crawford *et al.*, Adv. Colloid Interface Sci. **179–182**, 142 (2012). Copyright 2012, Elsevier.

A. Surface roughness

The relationship between surface roughness and bacterial adhesion has been studied extensively. To this day, two different mechanisms involving surface roughness have been proposed. Some scholars revealed that adhesion forces increased with increasing surface roughness and greater cell adhesion to rougher surfaces.[22–24] Nevertheless, others argued a contrary result that an increase of surface roughness did not influence or even inhibited the adhesion of bacteria.[25–28] These contradictory results showing the lack of consensus in terms of the relationship between surface roughness and bacterial adhesion could be attributed to the fact that the surface roughness parameters considered in the majority of studies do not describe comprehensive topographic characteristics of surfaces. Average surface roughness (R_a) and root-mean-square surface roughness (R_{rms}) are the most frequently used parameters for characterizing surface topography, and numerous efforts have been made to study the correlation between bacterial adhesion and these two parameters.[29–31] However, R_a and R_{rms} stand for the average and root-mean-square deviation of height values from the mean line, respectively, and both provide no information about the spatial distribution or shape of the surface features.[32] Surfaces with completely different surface structures may have similar R_a and R_{rms} values (Fig. 3). Accordingly, new parameters are needed for the comprehensive characterization of surface topography. Stout proposed a set of 14 roughness parameters for the comprehensive analysis of surfaces, which are referred to as "Birmingham 14" in the literature.[33] Crawford *et al.* selected three parameters from the Birmingham 14 as the minimum standard for surface topographical characterization in cell adhesion studies.[32] This new set of parameters consist of summit density (S_{ds}), which presents the number of summits per unit area; developed area ratio (S_{dr}), which presents the ratio of the surface area to the projected surface area; and

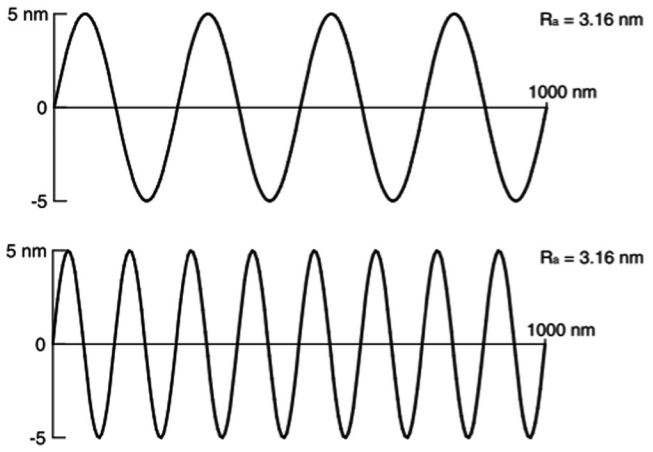

FIG. 3. Example of two different surfaces with identical R_a values. Reprinted from R. J. Crawford *et al.*, Adv. Colloid Interface Sci. **179–182**, 142 (2012). Copyright 2012, Elsevier.

root-mean-square surface roughness (R_{rms}). These parameters combined may offer insights into the shape and spatial distribution of surface features. As a consequence, controlling and designing of these surface features and patterns may become practicable. However, the effectiveness of this new set of parameters in comprehensively describing surface topography still remains to be verified.

B. Patterned surface topography

Various natural surfaces from animals and plants also present antifouling and self-cleaning properties, such as shark skin,[34–36] worm skin,[37] lotus leaves,[38] taro leaves,[39] butterfly wings,[40,41] and damselfly wings.[42] Enlightened by the natural surfaces, precise surfaces have been patterned for investigating cell-surface interactions and designing antibacterial surfaces due to the development of surface engineering technologies. The influences of plateau dimensions,[43] shapes and heights,[44] and spacing between the plateaus[45,46] on the attachment of bacteria were investigated. Polydimethylsiloxane (PDMS) is usually used material due to its innocuity, satisfied elasticity, and workability. Perera-Costa *et al.* produced protruded or recessed surface features of different shapes and heights on PDMS surfaces [Fig. 4(a)].[44] All patterned surfaces exhibited a significant overall reduction of bacterial adhesion compared to the flat surfaces. Hou *et al.* produced 10 μm tall square-shaped protruding features with different plateau dimensions on PDMS surfaces by soft lithography.[43] *E. coli* was observed to preferentially choose valleys between the square features to settle and form biofilms, even when the dimension of plateaus is considerably larger than that of valleys [Fig. 4(b)]. Friedlander *et al.* fabricated PDMS surfaces with arrays of hexagonal features with different spacing.[45] Bacterial adhesion on patterned surfaces was inhibited during the early stage but was then promoted compared to the flat surfaces. Gu *et al.* studied the adhesion behavior of *E. coli* on PDMS surfaces with 5 μm tall line patterns with different widths.[46] Narrow patterns with smaller interpattern spacing showed a more pronounced ability to inhibit bacterial adhesion.

Besides PDMS, other materials are also developed to pattern antibacterial surfaces. Jahed *et al.* investigated the adhesion of *S. aureus* on nanocrystalline nickle nanostructures with different shapes.[47] Bacterial cells were found to preferentially adhere to the interfaces of features and substrates or the conjunctions between different parts of features, where they were protected from external shear force and contact area was maximized [Fig. 4(c)]. Feng *et al.* produced nanopores of different diameters on alumina surfaces by anodization.[5] Anodized alumina surfaces with 15 or 25 nm pores exhibited reduced bacterial attachment and biofilm formation, while the surface with 100 nm pores promoted bacterial adhesion at a level even higher than the nanosmooth surface. Jin *et al.* fabricated polyethylene terephthalate (PET) nanopillar arrays with different interpillar spacing via reactive ion beam etching.[48] Bacterial adhesion was promoted when the interpillar spacing was much smaller than the diameter of bacterial cells and was inhibited when the interpillar spacing approached the diameter of bacterial cells. Furthermore, the presence of nanopillar arrays was found to change bacterial morphology, including diameter, length, and side curvature, indicating a possible correlation between bacterial adhesion and cell morphology.

Based on the outstanding research results mentioned above, some principles were proposed by researchers for designing surface topographies with the best antifouling performance, e.g., the height of surface features should exceed the length of flagella to prevent them from reaching into grooves;[46] the area of plateaus should be smaller than 20 μm × 20 μm in order to prevent severe biofilm formation.[43] These principles, however, are subject to the limited application due to biodiversity and the complexity of various environment.

The abovementioned studies demonstrate that precisely patterned surfaces are promising candidates for antifouling applications. Microscale surface topographic features may inhibit or promote bacterial adhesion and biofilm formation, depending on the size, shape, and density of the features. Further studies are needed to offer deeper insights into cell-surface interactions, including the mechanism by which surface topography influences the genomics and proteomics of bacterial cells.

III. BACTERICIDAL SURFACES

Bactericidal surfaces are the surfaces with an ability to kill or inactivate adhering bacterial cells.[49] In recent years, natural bactericidal surfaces have been discovered and the physical bactericidal mechanisms were also investigated.[49–60] Based on these physical bactericidal research, some artificial physical bactericidal surfaces have become the research focus. These surfaces possess nanoscale surface topographic features that can rupture the outer membrane of bacterial cells and in turn lead to cell death.

A. Natural bactericidal surfaces

Ivanova *et al.* first discovered the bactericidal properties of cicada (*Psaltoda claripennis*) wings when investigating

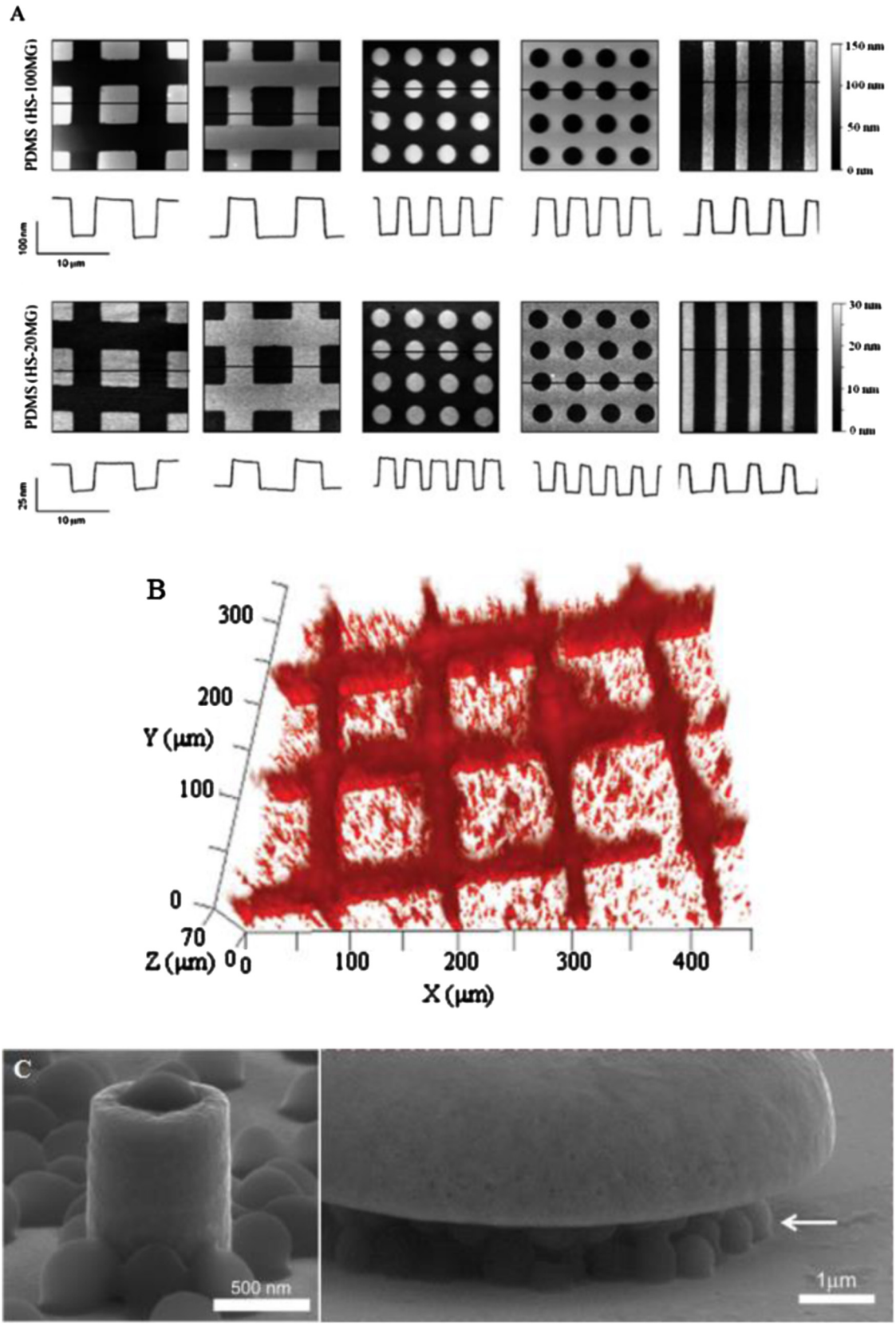

FIG. 4. (a) AFM images of the topographic features produced on PDMS surfaces. (b) Preference of *E. coli* adhesion on a patterned PDMS surface. Bacteria tended to choose valleys instead of protruding square features. (c) SEM micrographs showing the adhesion of *S. aureus* cells on nickel nanostructures. Reprinted (a) from D. Perera-Costa *et al*., Langmuir **30**, 4633 (2014). Copyright 2014, American Chemical Society. Reprinted (b) from S. Hou *et al*., Langmuir **27**, 2686 (2011). Copyright 2011, American Chemical Society. Reprinted (c) from Z. Jahed *et al*., Biomaterials **35**, 4249 (2014). Copyright 2014, Elsevier.

the antifouling ability of the wing surface.[50] Cicada wings were found to possess nanopillar arrays with approximately hexagonal spacing [Fig. 5(a)]. The nanopillars on the wings of *Psaltoda claripennis* are 200 nm in height, 100 and 60 nm in diameter at the base and top, respectively, with spacing of 170 nm from center to center. The nanopillars were found lethal to *Pseudomonas aeruginosa* cells, instantly penetrating them upon contact and effectively killing them within 5 min. The wings remained clean by killing attaching bacteria rather than repelling them. Altering surface chemistry of the wings by gold coating did not affect their bactericidal properties, suggesting that the bactericidal effect is a result of physical interactions instead of chemical reactions. To investigate the applicability of this effect to different bacterial species, Hasan *et al*. tested the bactericidal properties of *Psaltoda claripennis* wings against *B. subtilis*, *B. catarrhalis*, *E. coli*, *P. maritimus*, *P. aeruginosa*, *P. fluorescens*, and *S. aureus*.[49] It was found that the wings could effectively kill Gram-negative bacteria (*B. catarrhalis*, *E. coli*, *P. aeruginosa*, and *P. fluorescens*), while the viability of Gram-positive bacteria (*B. subtilis*, *P. maritimus*, and *S. aureus*) was not affected. Cell morphology did not seem to have any effect on cell viability. Kelleher *et al*. compared the bactericidal efficiency of the wings of three different cicada species (*Megapomponia intermedia*, *Ayuthia spectabile*, and *Cryptotympana aguila*) [Fig. 5(b)].[55] The wings of the three species all possess nanopillar arrays but with different heights, diameters, and spacing. The results show that the wings of *Megapomponia intermedia*, which have the nanopillars with the largest height, smallest diameter, and spacing, were most effective in killing Gram-negative *P. fluorescens*. The more pronounced bactericidal effect of *M. intermedia* wings can be primarily attributed to the sharper nanopillars inflicting a stronger stretching stimulus to bacteria. This phenomenon is also possibly linked to the greater height or smaller spacing. Pogodin *et al*. proposed a biophysical model to explain the interaction between bacterial cells and nanopillars on cicada wings [Figs. 5(c) and 5(d)].[54] Calculations demonstrated that as bacterial cells adsorbed onto nanopillars and sank deeper, the cell membrane suspended between two nanopillars was excessively stretched to a point of rupture, causing cell death. It was thus hypothesized that the cell membrane was not pierced by the nanopillars but ruptured between the nanopillars. Gram-positive bacteria, however, were resistant to this physical effect due to their thicker and more rigid cell membrane. After decreasing the rigidity of their cell membrane by microwave treatment, Gram-positive bacteria were rendered susceptible to the bactericidal effect of cicada wings. Xue *et al*. proposed another model claiming that the physical interaction between bacterial cells and nanopillars on cicada wings cannot provide sufficient energy to cause cell rupture.[59] Gravity and nonspecific forces such as van der Waals forces may play a role in the rupture of cell membrane. Apart from cicada wings, dragonfly wings were also found to possess bactericidal properties. Ivanova *et al*. discovered that the wings of the dragonfly *Diplacodes bipunctata* can effectively kill not only both Gram-negative (*P. aeruginosa*) and Gram-positive (*S. aureus* and *B. subtilis*) bacterial cells but also *B. subtilis* spores.[56] Dragonfly wings also possess nanopillars similar to those of cicada wings but with a random size, shape, and spatial distribution [Fig. 5(e)]. Complex nanopillar clusters were observed on the dragonfly wing surface while cicada wings possess regular arrays of nanopillars. Bandara *et al*. proposed another mechanism when studying the bactericidal effects of dragonfly wings on *E. coli*.[60] Bacterial cell membrane damage is possibly initiated by the strong adhesion between EPSs and nanopillars, as well as the shear force generated when immobilized bacteria try to move away. Watson *et al*. found that the skin of the gecko *L. steindachneri* has bactericidal function on Gram-negative bacteria (*P. gingivalis*).[57] Spherically capped nanoscale spinules with a high density were observed on gecko skin [Fig. 5(f)] that were found to kill Gram-negative bacteria and promote the growth of eukaryotic cells. Li *et al*. further investigated cell-surface interaction on gecko skin.[58] Both Gram-positive (*S. mutans*) and Gram-negative (*P. gingivalis*) bacteria were found susceptible to the bactericidal effect of the spinules, but more pronounced effect was observed on Gram-negative *P. gingivalis*. The relatively larger *P. gingivalis* cells were directly penetrated by the spinules while the smaller *S. mutans* cells were more likely to settle between the spinules. This direct piercing mechanism was also observed by Deokar *et al*. who found that *S. aureus* and *E. coli* bacteria were directly penetrated by single-walled carbon nanotubes.[61] An alternative bactericidal mechanism was proposed for the cells settled between the spinules, where they experienced compression or stretching by the side of spinules that led to cell damage and death. Moreover, a riblike structure was found on the underlying surface where the spinules are based. The riblike structure and the spinules form a hierarchical topography that synergistically impair or kill bacteria.

A wide variety of animals and plants possess antifouling or bactericidal properties to protect them from contamination of bacteria, fungi, plants, and abiotic particles. Some natural surfaces present both properties at the same time. Superhydrophobicity allows these surfaces to wash away contaminants with water droplets, while nanopillar structures enable them to kill attaching bacterial cells. Nature is always a rich source of innovation, and extensive work is needed to imitate the naturally evolved surface structures for enhanced antibacterial performances.

B. Artificial bactericidal surfaces

Inspired by naturally evolved surfaces, a variety of biomimetic surfaces have been developed to achieve bactericidal properties. Ivanova *et al*. produced nanopillars on the surface of black silicon (bSi) by reactive ion etching [Fig. 6(a)].[56] Gram-negative (*P. aeruginosa*), Gram-positive (*S. aureus* and *B. subtilis*) bacterial cells and *B. subtilis* spores were killed with a high efficiency by black silicon, at approximately the same rate as that achieved by dragonfly wings. In another study, black silicon surfaces were preinfected with

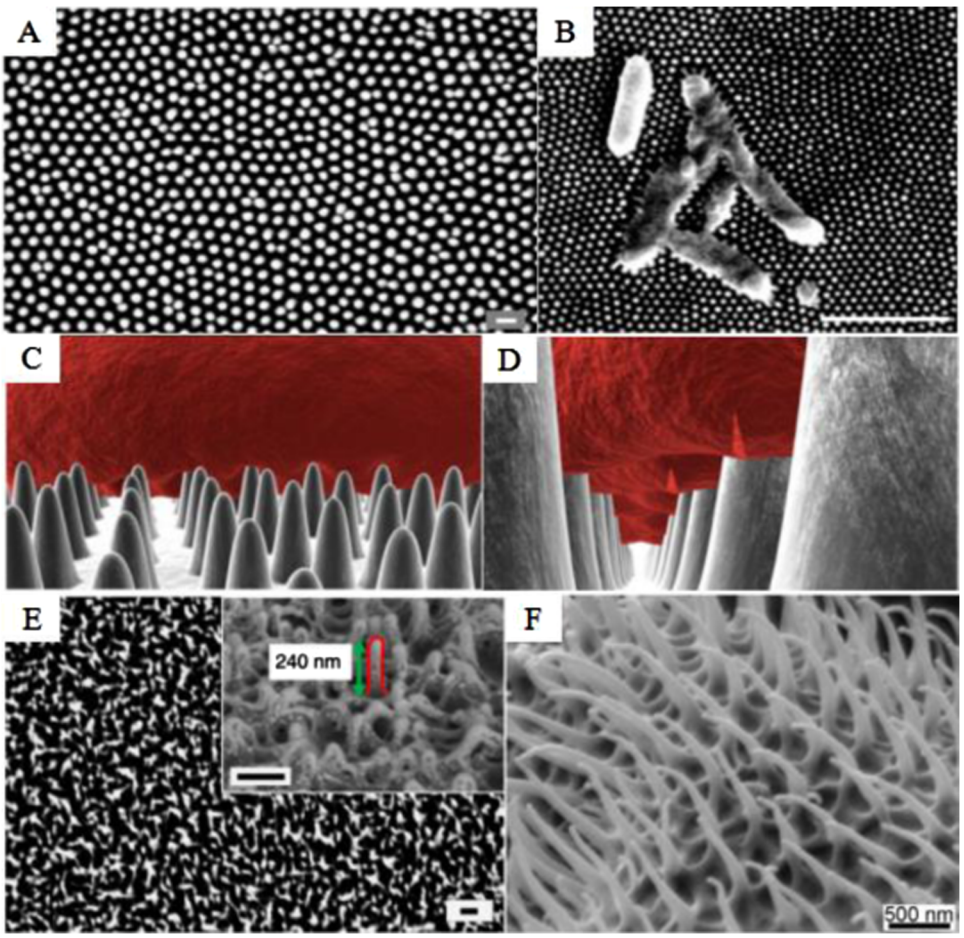

FIG. 5. (a) Nanopillars on a cicada wing surface. (b) An SEM image showing *P. fluorescens* bacteria ruptured and killed by the nanopillars of *Megapomponia intermedia* cicada wing. [(c) and (d)] A biophysical model of bacterial cells being ruptured by cicada wing nanopillars. (e) Nanopillars on a dragonfly wing surface. (f) Nanospinules on a gecko skin surface. Reprinted (a), (c), and (d) from S. Pogodin *et al.*, Biophys. J. **104**, 835 (2013). Copyright 2013, Biophysical Society. Reprinted (b) from S. M. Kelleher *et al.*, ACS Appl. Mater. Interfaces **8**, 14966 (2016). Copyright 2016, American Chemical Society. Reprinted (e) from E. P. Ivanova *et al.*, Nat. Commun. **4**, 2838 (2013). Copyright 2013, Macmillan Publishers Limited. Reprinted (f) from G. S. Watson *et al.*, Acta Biomater. **21**, 109 (2015). Copyright 2015, Elsevier.

P. aeruginosa or *S. aureus* cells, and then, fibroblast cells were incubated on these surfaces to study the competitive colonization between eukaryotic cells and bacterial cells.[62] Fibroblast cells successfully grew and proliferated on black silicon surfaces while bacterial cells were ruptured and killed by the nanopillars. Linklater *et al.* produced three types of black silicon surfaces with different nanopillar heights, diameters, and spacing by varying etching intervals.[63] All three

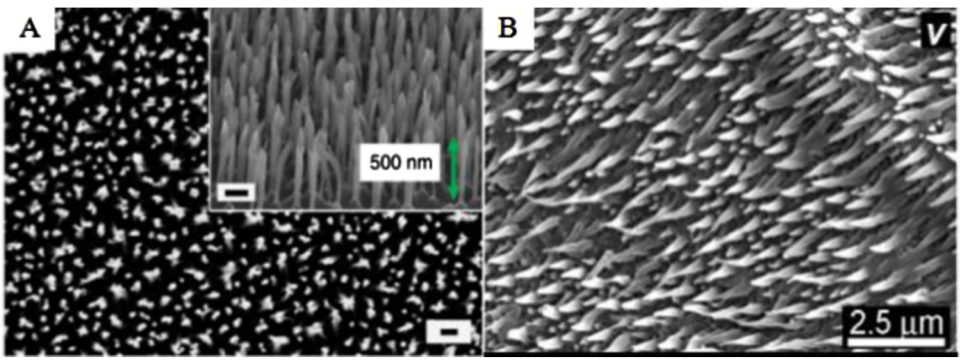

FIG. 6. (a) Nanopillars on a black silicon surface. (b) Nanoscale spinules on a polystyrene gecko skin replica surface. Reprinted (a) from E. P. Ivanova *et al.*, Nat. Commun. **4**, 2838 (2013). Copyright 2013, Macmillan Publishers Limited. Reprinted (b) from D. W. Green *et al.*, Sci. Rep. **7**, 41023 (2017). Copyright 2017, Macmillan Publishers Limited.

surfaces achieved lower adhesion rates and cell viability compared to the nonstructured silicon wafer surface. Nanopillars of the lowest height, smallest diameter, and interpillar spacing were found to be more effective at killing Gram-positive (*S. aureus*) and Gram-negative (*P. aeruginosa*) bacteria. Green *et al*. replicated the spinules of gecko skin onto epoxy resin and obtained synthetic spinules slightly shorter than natural ones [Fig. 6(b)].[64] The bactericidal effect of the replica surface was similar to that of the natural gecko skin, effectively killing both Gram-positive (*S. mutans*) and Gram-negative (*P. gingivalis*) bacteria.

Bactericidal properties can also be achieved on metallic surfaces. Sengstock *et al*. fabricated nanocolumnar titanium (Ti) thin films on silicon substrates by glancing angle sputter deposition.[65] Cell viability of Gram-negative *E. coli* on the nanopatterned Ti surface substantially decreased compared to that on the dense Ti surface, but the viability of Gram-positive *S. aureus* was not affected. Bhadra *et al*. produced nanowire arrays on Ti surfaces by hydrothermal etching.[66] The nanopatterned surfaces were effective at killing both Gram-positive (*S. aureus*) and Gram-negative (*P. aeruginosa*) bacteria by causing cell wall deformation and rupture. Wu *et al*. fabricated gold (Au) nanopillars, nanorings, and nanonuggets on tungsten substrates by electrodeposition.[67] Surfaces with the three types of nanoprotrusions demonstrated similar bactericidal efficiency (more than 99%) in killing *S. aureus* cells. Linklater *et al*. fabricated surfaces with vertically aligned high aspect ratio carbon nanotubes and proposed a new bactericidal mechanism.[68] It was found that the release of elastic energy previously stored in the nanotubes upon contact with bacterial cells could stretch cell membrane and cause cell death.

IV. SURFACE CONSTRUCTION METHODS

After years of extensive studies, the mechanisms of bacteria/surface interactions and antibacterial surface topographies have been gradually revealed. Precise and cost-efficient surface construction methods are needed to produce synthetic surface topographies for optimized antibacterial performances. A variety of methods have been applied to roughen surfaces, produce micro- and nanoscale surface patterns, or imitate/replicate natural surface topographies.

A. Surface roughening methods

Severe plastic deformation is one way to increase microscale surface roughness of metallic surfaces. Equal channel angular pressing (ECAP) is a method used to strengthen metallic materials, with a side effect of increasing microscale surface roughness. Truong *et al*. found that bacterial adhesion was promoted on ECAP modified Ti surfaces.[22] Severe shot peening (SSP) is another example of severe plastic deformation technique, namely, impacting the material surface with high energy shots.[25] Sharma *et al*. altered the subnanoscale roughness of glass surfaces by surface silanization.[24] Preedy *et al*. varied surface roughness of borosilicate glass by grinding the surface with abrasive particles of different sizes.[23] This method is simple and causes no variation of surface chemistry or grain size. Chen *et al*. produced flame-sprayed Al coatings with surface asperities by employing stainless steel mesh with the size of 125 μm as a shielding plate during coating deposition.[69] Asperities with the size of ~150 μm in diameter and ~70 μm in height were fabricated on the surfaces of the coatings [Figs. 7(a) and 7(b)]. Liu *et al*. roughened PDMS surface using a template method [Fig. 7(c)].[26] Ti was used as the template and processed with electrochemical anodization to create nanotubular structures. Different degrees of surface roughness were obtained by adjusting anodization voltage. Lüdecke *et al*. produced Ti thin films on glass slides by physical vapor deposition.[27] Surface roughness was adjusted by changing deposition rate and film thickness. Rizzello *et al*. fabricated nanorough Au surfaces using spontaneous galvanic displacement reaction.[28]

The challenge for surface roughening is altering surface roughness without changing other surface properties such as grain size and surface chemistry, which may involve side effects. For instance, ECAP and SSP are often used to alter surface roughness, however in which grain size is also reduced.[22,25] Another example is surface silanization by assembling organosilane layers bearing carbon chains with different lengths on glass surfaces.[24] However, the difference in surface chemistry might have also played a role in bacterial adhesion because the carbon chains carried different functional groups. Therefore, additional processing may be needed to remove the influence of these side effects.

B. Surface patterning methods

Many technologies were proposed for producing surface topographic patterns with various sizes, shapes, and spatial distributions. Techniques based on replication are commonly used methods to produce micro- and nanoscale topographic features on polymer surfaces, e.g., PDMS, poly(urethane urea), and poly(methyl methacrylate).[43–46,64,70–84] Such replication methods include soft lithography, biotemplating methods,[64,75,76] and nanoimprinting.[77–81] Green *et al*. replicated the nanostructures of gecko skin on multiple synthetic biomaterial surfaces using a biotemplating method.[64] Nanoimprinting, also known as hot embossing, is a type of lithography that uses a mold to replicate nanostructures to a surface.[81] Hong *et al*. duplicated the nanopillars of cicada wings by UV nanoimprinting.[79] Polymer surface patterning can also be achieved using direct laser interference patterning (DLIP). Valle *et al*. successfully created linelike, pillarlike, and lamellalike structures on polystyrene, polyimide, and PET surfaces by DLIP.[85]

Besides replication methods, there are also some other technologies reported to fabricate patterned surfaces. Reactive ion etching is a technique used to fabricate nanostructures by bombarding high energy ions onto material surfaces to achieve material removal.[86] This method is usually used to treat black silicon surfaces,[56,62,63,87–90] PET surfaces,[47] and diamond surfaces.[91] Besides reactive ion etching, photolithography, dry etching, and laser ablation are

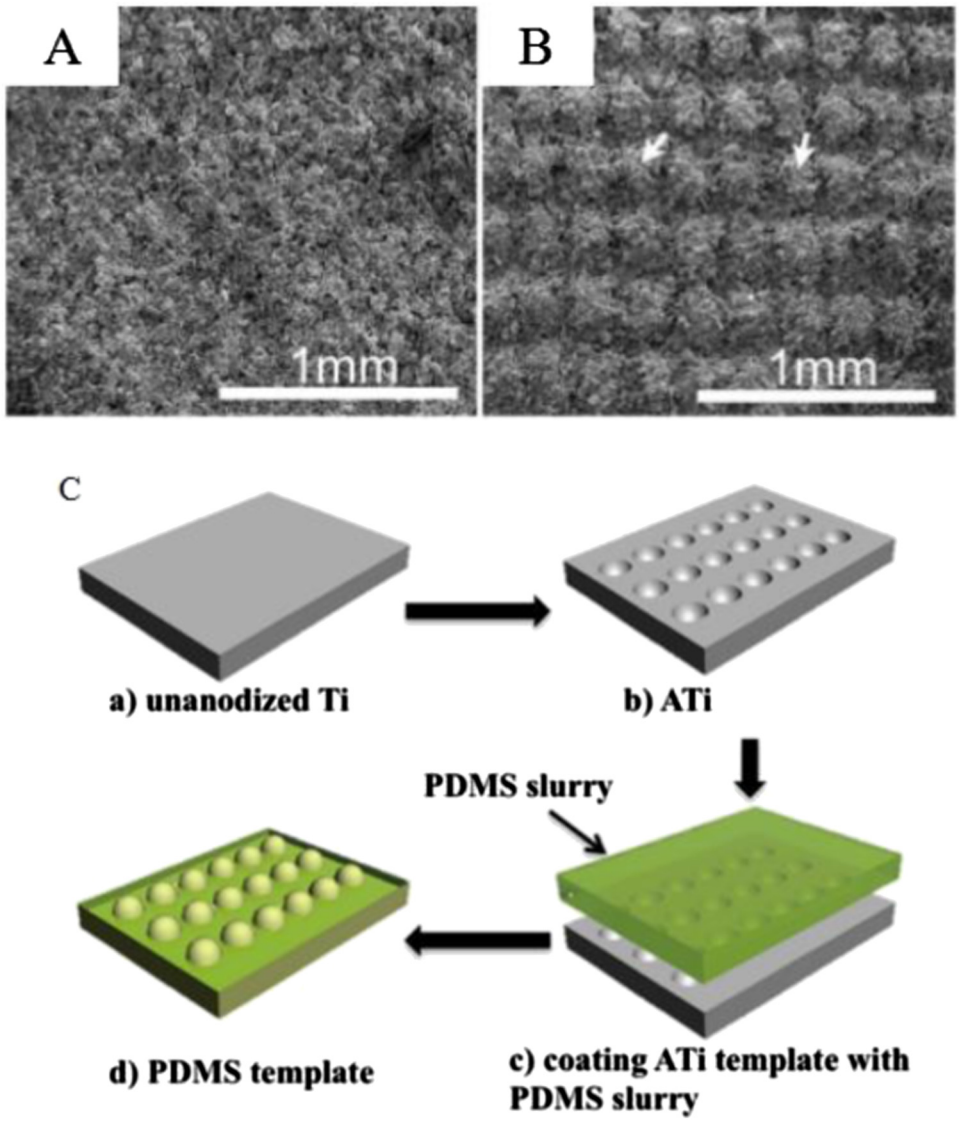

FIG. 7. (a) and (b) Comparison between flame-sprayed flat Al coating surface and micropatterned Al coating surface with asperities. (c) The process of fabricating nanostructures on PDMS surfaces. Reprinted (a) and (b) from X. Chen *et al.*, Appl. Surf. Sci. **388**, 385 (2015). Copyright 2015, Elsevier. Reprinted (c) from L. Liu *et al.*, ACS Biomater. Sci. Eng. **2**, 122 (2016). Copyright 2016, American Chemical Society.

also commonly used ways to produce nanoscale surface topographic features on silicon surfaces.[92–94]

On metal surfaces, various ways have also been developed to effectively produce patterns. Anodization is a method for creating nanopores on metallic oxide surfaces.[5,26,95] Feng *et al.* produced nanopores on alumina surfaces by a two-step anodization process of Al.[5] Sjöström *et al.* fabricated bactericidal nanospikes on Ti alloy surfaces via thermal oxidation.[96] The geometry of nanospikes was tuned by adjusting acetone vapor concentration. Chemical etching is another frequently utilized method to produce surface structures on Ti surfaces.[66,97–101] Bhadra *et al.* produced nanowires on Ti surfaces using hydrothermal etching.[66] Ti substrates were fully immersed in a KOH solution and subjected to a high temperature and high pressure treatment for 1 h, followed by an additional heat treatment. Diu *et al.* created two types of titania nanowire arrays using hydrothermal etching.[97] Luo *et al.* produced a hierarchical structure consisting of micropits and nanostructures on Ti surfaces by sandblasting and chemical etching.[98] Zhu *et al.* produced a homogeneous porous nanostructure on Ti surfaces using acid etching and H_2O_2 aging.[99] Sengstock *et al.* fabricated nanocolumnar Ti thin films on silicon substrates by glancing angle sputter deposition.[65] Jahed *et al.* fabricated nanocrystalline nickel nanoscale features using electron beam lithography.[47] Wu *et al.* produced Au nanostructures by templated electrodeposition.[67] Femtosecond laser ablation is another method widely applied to fabricate surface patterns on metal surfaces. Cunha *et al.* produced periodic surface structures and nanopillars on grade 2 Ti alloy surfaces.[102] Epperlein *et al.* produced periodic surface structures on the surfaces of structural steel and stainless steel.[103] Fadeeva *et al.* and Truong *et al.* created hierarchical structures mimicking lotus leaf surface on Ti surfaces using femtosecond laser ablation.[104,105] Serrano *et al.*

successfully created nanolamellae on medical sutures using plasma treatment.[106] Lamellae sizes were adjusted by altering plasma treatment time. Pham *et al*. produced antibacterial graphene film surfaces with multiple layers of graphene nanosheets.[107] Graphene was produced using liquid-phase exfoliation, and then the graphene films were subsequently produced by vacuum filtration. Other methods such as colloidal lithography, focused ion beam milling, and electron beam lithography are also promising candidates for producing micro- and nanoscale surface patterns for antimicrobial purposes.[108–110]

To summarize, the abovementioned techniques can be classified into three categories: replication, high energy surface patterning, and chemical patterning. Replication methods allow fast duplication of fine patterns onto soft polymer surfaces with excellent accuracy and precision. High energy surface patterning methods including RIE, laser ablation, and photolithography are applicable to a wide range of materials. Surface chemical patterning methods possess the advantage of cost effectiveness, ease of use, high throughput, and applicability on an industrial scale.

V. CONCLUSIONS AND PERSPECTIVES

Recent years of research have brought the understanding of cell-surface interaction and the design of the antibacterial surface topography to a new level. Some surfaces with micro- or nanoscale surface features present enhanced antibacterial properties, either by preventing bacterial adhesion or by killing/inactivating adherent bacteria. Since incomprehensive surface roughness parameters have failed to precisely characterize surface topography, patterned surfaces have become the new research frontier. Inspired by nature, bactericidal surfaces with high aspect ratio nanopillars have been developed, which provide an alternative way to kill bacteria without surface chemical modification. Various techniques have been developed to fabricate surface features and remain to be further applied to the design and production of antibacterial surfaces.

In real marine or *in vivo* environment, the surfaces of marine vehicles, industrial facilities, and medical implants face consecutive colonizing attempts of bacteria. Some bacterial species excrete EPSs to enhance adhesion and form biofilms. EPS also change the surface topography by filling or covering surface topographic features. The long-term antibacterial properties of surface topographies after being changed by EPS need to be extensively studied. In addition, the majority of current research only focuses on single bacterial species, whereas real biofilms are composed of multiple species, cohabiting with or competing against each other. Surface topographies pose different effects to different species and influence interspecies interactions. Extensive research is needed to deepen the understanding of these interactions and pave the way for application in the medical and marine industries. Moreover, the majority of current research was conducted *in vitro*, and *in vivo* studies are needed in order to achieve application in the medical industry.

ACKNOWLEDGMENTS

This work was supported by the National Natural Science Foundation of China (Grant No. 21705158), the Key Research and Development Program of Zhejiang Province (No. 2015C01036), the International Scientific and Technological Cooperation Project of Ningbo (No. 2017D10011), the Fundamental Research Project of Qinghai Province (No. 2016ZJ757), and the 3315 Program of Ningbo.

[1]D. M. Yebra, S. Kiil, and K. Dam-Johansen, Prog. Org. Coat. **50**, 75 (2004).
[2]M. Lejars, A. Margaillan, and C. Bressy, Chem. Rev. **112**, 4347 (2012).
[3]T. Yamamoto, C. Emura, and M. Oya, Comput. Biol. Med. **79**, 173 (2016).
[4]A. Bhattacharjee, M. Khan, M. Kleiman, and A. I. Hochbaum, ACS Appl. Mater. Interfaces **9**, 18531 (2017).
[5]G. Feng, Y. Cheng, S. Wang, L. Hsu, Y. Feliz, D. A. Borca-Tasciuc, R. W. Worobo, and C. I. Moraru, Biofouling **30**, 1253 (2014).
[6]L. H. Koole and M. L. W. Knetsch, Polymers **3**, 340 (2011).
[7]P. J. Kelly, H. Li, K. A. Whitehead, J. Verran, R. D. Arnell, and I. Iordanova, Surf. Coat. Technol. **204**, 1137 (2009).
[8]O. Gordon, T. V. Slenters, P. S. Brunetto, A. E. Villaruz, D. E. Sturdevant, M. Otto, R. Landmann, and K. M. Fromm, Antimicrob. Agents Chemother. **54**, 4208 (2010).
[9]Y. Liu, X. Suo, Z. Wang, Y. Gong, X. Wang, and H. Li, Mater. Des. **130**, 285 (2017).
[10]Z. Jia, Y. Liu, Y. Wang, Y. Gong, P. Jin, X. Suo, and H. Li, Surf. Coat. Technol. **309**, 872 (2017).
[11]L. V. Stamm, Antimicrob. Agents Chemother. **54**, 583 (2010).
[12]A. D. Harris *et al.*, Antimicrob. Agents Chemother. **54**, 3143 (2010).
[13]Z. Cao, L. Mi, J. Mendiola, J. Ella-Menye, L. Zhang, H. Xue, and S. Jiang, Angew. Chem. Int. Ed. **51**, 2602 (2012).
[14]X. Dou, D. Zhang, C. Feng, and L. Jiang, ACS Nano. **9**, 10664 (2015).
[15]A. K. Epstein, T. S. Wong, R. A. Belisle, E. M. Boggs, and J. Aizenberg, Proc. Natl. Acad. Sci. U.S.A. **109**, 13182 (2012).
[16]E. P. Ivanova, V. K. Truong, H. K. Webb, V. A. Baulin, J. Wang, N. Mohammodi, F. Wang, C. J. Fluke, and R. J. Crawford, Sci. Rep. **1**, 165 (2011).
[17]X. Zhang, L. Wang, and E. Levanen, RSC Adv. **3**, 12003 (2013).
[18]P. Tang, W. Zhang, Y. Wang, B. Zhang, H. Wang, C. Lin, and L. Zhang, J. Nanomater. **2011**, 178921.
[19]B. J. Privett, J. Youn, S. A. Hong, J. Lee, J. Han, J. H. Shin, and M. H. Schoenfisch, Langmuir **27**, 9597 (2011).
[20]C. R. Crick, S. Ismail, J. Pratten, and I. P. Parkin, Thin Solid Films. **519**, 3722 (2011).
[21]L. R. Freschauf, J. McLane, H. Sharma, and M. Khine, PLoS One **7**, 40987 (2012).
[22]V. K. Truong, R. Lapovok, Y. S. Estrin, S. Rundell, J. Wang, C. J. Fluke, R. J. Crawford, and E. P. Ivanova, Biomaterials **31**, 3674 (2010).
[23]E. Preedy, S. Perni, D. Nipic, K. Bohinc, and P. Prokopovich, Langmuir **30**, 9466 (2014).
[24]S. Sharma, Y. A. Jaimes-Lizcano, R. B. McLay, P. C. Cirino, and J. C. Conrad, Langmuir **32**, 5422 (2016).
[25]S. Bagherifard, D. J. Hickey, A. C. de Luca, V. N. Malheiro, A. E. Markaki, M. Guagliano, and T. J. Webster, Biomaterials **73**, 185 (2015).
[26]L. Liu, B. Ercan, L. Sun, K. S. Ziemer, and T. J. Webster, ACS Biomater. Sci. Eng. **2**, 122 (2016).
[27]C. Lüdecke, M. Roth, W. Yu, U. Horn, J. Bossert, and K. D. Jandt, Colloids Surf. B: Biointerfaces **145**, 617 (2016).
[28]L. Rizzello, B. Sorce, S. Sabella, G. Vecchio, A. Galeone, V. Brunetti, R. Cingolani, and P. P. Pompa, ACS Nano **5**, 1865 (2011).
[29]V. K. Truong, J. Wang, R. Lapovok, Y. Estrin, F. Malherbe, C. Berndt, R. J. Crawford, and E. P. Ivanova, Prog. Colloid Polym. Sci. **137**, 41 (2010).
[30]Y. H. An, R. J. Friedman, R. A. Draughn, E. A. Smith, J. H. Nicholson, and J. F. John, J. Microbiol. Methods **24**, 29 (1995).
[31]K. A. Whitehead, D. Rogers, J. Colligon, C. Wright, and J. Verran, Colloids Surf. B: Biointerfaces **51**, 44 (2006).

[32]R. J. Crawford, H. K. Webb, V. K. Truong, J. Hasan, and E. P. Ivanova, Adv. Colloid Interface Sci. **179–182**, 142 (2012).
[33]K. J. Stout, *Development of Methods for the Characterisation of Roughness in Three Dimensions* (Elsevier Science and Technology, Amsterdam, 1993).
[34]A. Sakamoto *et al.*, FEMS Microbiol. Lett. **361**, 1 (2014).
[35]C. M. Magin, S. P. Cooper, and A. B. Brennan, Mater. Today **13**, 4 (2010).
[36]K. K. Chung, J. F. Schumacher, E. M. Sampson, R. A. Burne, P. J. Antonelli, and A. B. Brennan, Biointerphases **2**, 2 (2007).
[37]M. J. Hayes, T. P. Levine, and R. H. Wilson, J. Insect Sci. **16**, 1 (2016).
[38]A. Solga, Z. Cerman, B. F. Striffler, M. Spaeth, and W. Barthlott, Bioinspir. Biomim. **2**, 4 (2007).
[39]J. Ma, Y. Sun, K. Gleichauf, J. Lou, and Q. Li, Langmuir **27**, 10035 (2011).
[40]Y. Fang and G. Sun, Appl. Mech. Mater. **723**, 943 (2014).
[41]G. D. Bixler and B. Bhushan, Nanoscale **6**, 76 (2013).
[42]J. Hasan *et al.*, Langmuir **28**, 17404 (2012).
[43]S. Hou, H. Gu, C. Smith, and D. Ren, Langmuir **27**, 2686 (2011).
[44]D. Perera-Costa, J. M. Bruque, M. L. Gonzalez-Martin, A. C. Gomez-Garcia, and V. Vadillo-Rodriguez, Langmuir **30**, 4633 (2014).
[45]R. S. Friedlander, H. Vlamakis, P. Kim, M. Khan, R. Kolter, and J. Aizenberg, Proc. Natl. Acad. Sci. U.S.A. **110**, 5624 (2013).
[46]H. Gu, A. Chen, X. Song, M. E. Brasch, J. H. Henderson, and D. Ren, Sci. Rep. **6**, 29516 (2016).
[47]Z. Jahed, P. Lin, B. B. Seo, M. S. Verma, F. Gu, T. Tsui, and M. R. Mofrad, Biomaterials **35**, 4249 (2014).
[48]L. Jin, W. Guo, P. Xue, H. Gao, M. Zhao, C. Zheng, Y. Zhang, and D. Han, Nanotechnology **26**, 055702 (2015).
[49]J. Hasan, H. K. Webb, V. K. Truong, S. Pogodin, V. A. Baulin, G. S. Watson, J. A. Watson, R. J. Crawford, and E. P. Ivanova, Appl. Microbiol. Biotechnol. **97**, 9257 (2013).
[50]E. P. Ivanova *et al.*, Small **8**, 2489 (2012).
[51]K. Nowlin, A. Boseman, A. Covell, and D. LaJeunesse, J. R. Soc. Interface **12**, 0999 (2015).
[52]V. K. Truong, N. M. Geeganagamage, V. A. Baulin, J. Vongsvivut, M. J. Tobin, P. Luque, R. J. Crawford, and E. P. Ivanova, Appl. Microbiol. Biotechnol. **101**, 1 (2017).
[53]D. E. Mainwaring *et al.*, Nanoscale **8**, 6527 (2016).
[54]S. Pogodin *et al.*, Biophys. J. **104**, 835 (2013).
[55]S. M. Kelleher, O. Habimana, J. Lawler, B. O. Reilly, S. Daniels, E. Casey, and A. Cowley, ACS Appl. Mater. Interfaces **8**, 14966 (2016).
[56]E. P. Ivanova *et al.*, Nat. Commun. **4**, 2838 (2013).
[57]G. S. Watson, D. W. Green, L. Schwarzkopf, X. Li, B. W. Cribb, S. Myhra, and J. A. Watson, Acta Biomater. **21**, 109 (2015).
[58]X. Li, G. S. Cheung, G. S. Watson, J. A. Watson, S. Lin, L. Schwarzkopf, and D. W. Green, Nanoscale **8**, 18860 (2016).
[59]F. Xue, J. Liu, L. Guo, L. Zhang, and Q. Li, J. Theor. Biol. **385**, 1 (2015).
[60]C. D. Bandara, S. Singh, I. O. Afara, A. Wolff, T. Tesfamichael, K. Ostrikov, and A. Oloyede, ACS Appl. Mater. Interfaces **9**, 6746 (2017).
[61]A. R. Deokar, L. Lin, C. Chang, and Y. Ling, J. Mater. Chem. B **1**, 2639 (2013).
[62]V. T. Pham *et al.*, ACS Appl. Mater. Interfaces **8**, 22025 (2016).
[63]D. P. Linklater, H. K. D. Nguyen, C. M. Bhadra, S. Juodkazis, and E. P. Ivanova, Nanotechnology **28**, 245301 (2017).
[64]D. W. Green, K. K. Lee, J. A. Watson, H. Y. Kim, K. S. Yoon, E. J. Kim, J. M. Lee, G. S. Watson, and H. S. Jung, Sci. Rep. **7**, 41023 (2017).
[65]C. Sengstock, M. Lopian, Y. Motemani, A. Borgmann, C. Khare, P. J. Buenconsejo, T. A. Schildhauer, A. Ludwig, and M. Koller, Nanotechnology **25**, 195101 (2014).
[66]C. M. Bhadra, V. K. Truong, V. T. Pham, M. A. Kobaisi, G. Seniutinas, J. Wang, S. Juodkazis, R. J. Crawford, and E. P. Ivanova, Sci. Rep. **5**, 16817 (2015).
[67]S. Wu, F. Zuber, J. Brugger, K. Maniura-Weber, and Q. Ren, Nanoscale **8**, 2620 (2016).
[68]D. P. Linklater *et al.*, ACS Nano **12**, 6657 (2018).
[69]X. Chen, X. He, X. Suo, J. Huang, Y. Gong, Y. Liu, and H. Li, Appl. Surf. Sci. **388**, 385 (2015).
[70]H. Gu, S. Hou, C. Yongyat, S. De Tore, and D. Ren, Langmuir **29**, 11145 (2013).
[71]G. D. Bixler, A. Theiss, B. Bhushan, and S. C. Lee, J. Colloid Interface Sci. **419**, 114 (2014).
[72]N. Lu, W. Zhang, Y. Weng, X. Chen, Y. Cheng, and P. Zhou, Food Control **68**, 344 (2016).
[73]R. Vasudevan, A. J. Kennedy, M. Merritt, F. H. Crocker, and R. H. Baney, Colloids Surf. B: Biointerfaces **117**, 225 (2014).
[74]L. Xu and C. A. Siedlecki, Acta Biomater. **8**, 72 (2012).
[75]B. Zhang *et al.*, ACS Appl. Mater. Interfaces **6**, 12467 (2014).
[76]D. Zhang, Y. Li, X. Han, X. Li, and H. Chen, Chin. Sci. Bull. **56**, 938 (2011).
[77]M. N. Dickson, E. I. Liang, L. A. Rodriguez, N. Vollereaux, and A. F. Yee, Biointerphases **10**, 021010 (2015).
[78]S. Kim, U. T. Jung, S. K. Kim, J. H. Lee, H. S. Choi, C. S. Kim, and M. Y. Jeong, ACS Appl. Mater. Interfaces **7**, 326 (2015).
[79]S. Hong, J. Hwang, and H. Lee, Nanotechnology **20**, 385303 (2009).
[80]J. Y. Cho, G. Kim, S. Kim, and H. Lee, Electron. Mater. Lett. **9**, 523 (2013).
[81]A. Jaggessar, H. Shahali, A. Mathew, and P. K. D. V. Yarlagadda, J. Nanobiotechnol. **15**, 64 (2017).
[82]A. I. Hochbaum and J. Aizenberg, Nano Lett. **10**, 3717 (2010).
[83]Y. Liu and G. Li, J. Colloid Interface Sci. **388**, 235 (2012).
[84]D. Zhao, Z. Huang, M. Wang, T. Wang, and Y. Jin, J. Mater. Process. Technol. **212**, 198 (2012).
[85]J. Valle, S. Burgui, D. Langheinrich, C. Gil, C. Solano, A. Toledo-Arana, R. Helbig, A. Lasagni, and I. Lasa, Macromol. Biosci. **15**, 1060 (2015).
[86]S. Franssila, *Introduction to Microfabrication* (Wiley, New York, 2010).
[87]J. Hasan, S. Raj, L. Yadav, and K. Chatterjee, RSC Adv. **5**, 44953 (2015).
[88]F. Hizal, C. H. Choi, H. J. Busscher, and H. C. van der Mei, ACS Appl. Mater. Interfaces **8**, 30430 (2016).
[89]M. Yang, Y. Ding, X. Ge, and Y. Leng, Colloids Surf. B: Biointerfaces **135**, 549 (2015).
[90]P. W. May *et al.*, J. Mater. Chem. B **4**, 5737 (2016).
[91]L. E. Fisher, Y. Yang, M. Yuen, W. Zhang, A. H. Nobbs, and B. Su, Biointerphases **11**, 011014 (2016).
[92]X. Ge, Y. Leng, X. Lu, F. Ren, K. Wang, Y. Ding, and M. Yang, J. Biomed. Mater. Res. A **103**, 384 (2015).
[93]L. C. Hsu, J. Fang, D. A. Borca-Tasciuc, R. W. Worobo, and C. I. Moraru, Appl. Environ. Microbiol. **79**, 2703 (2013).
[94]S. Perni and P. Prokopovich, Soft Matter **9**, 1844 (2013).
[95]S. D. Puckett, E. Taylor, T. Raimondo, and T. J. Webster, Biomaterials **31**, 706 (2010).
[96]T. Sjöström, A. H. Nobbs, and B. Su, Mater. Lett. **167**, 22 (2016).
[97]T. Diu, N. Faruqui, T. Sjöström, B. Lamarre, H. F. Jenkinson, B. Su, and M. G. Ryadnov, Sci. Rep. **4**, 7122 (2014).
[98]Q. Luo, Y. Huang, G. Zha, Y. Chen, X. Deng, K. Zhang, W. Zhu, S. Zhao, and X. Li, J. Mater. Chem. B **3**, 784 (2015).
[99]C. Zhu, N. Bao, S. Chen, and J. Zhao, Appl. Surf. Sci. **389**, 7 (2016).
[100]P. M. Tsimbouri, L. Fisher, N. Holloway, T. Sjostrom, A. H. Nobbs, R. M. D. Meek, B. Su, and M. J. Dalby, Sci. Rep. **6**, 36857 (2016).
[101]M. Lorenzetti, I. Dogsa, T. Stosicki, D. Stopar, M. Kalin, S. Kobe, and S. Novak, ACS Appl. Mater. Interfaces **7**, 1644 (2015).
[102]A. Cunha, A. Elie, L. Plawinski, A. P. Serro, A. M. B. do Rego, A. Almeida, M. C. Urdaci, M. Durrieu, and R. Vilar, Appl. Surf. Sci. **360**, 485 (2016).
[103]N. Epperlein, F. Menzel, K. Schwibbert, R. Koter, J. Bonse, J. Sameith, J. Krüger, and J. Toepel, Appl. Surf. Sci. **418**, 420 (2017).
[104]E. Fadeeva, V. K. Truong, M. Stiesch, B. N. Chichkov, R. J. Crawford, J. Wang, and E. P. Ivanova, Langmuir **27**, 3012 (2011).
[105]V. K. Truong, H. K. Webb, E. Fadeeva, B. N. Chichkov, A. Wu, R. Lamb, J. Wang, R. J. Crawford, and E. P. Ivanova, Biofouling **28**, 539 (2012).
[106]C. Serrano *et al.*, Biomaterials **52**, 291 (2015).
[107]V. H. Pham, V. K. Truong, M. D. J. Quinn, S. M. Notley, Y. Guo, V. A. Baulin, M. A. Kobaisi, R. J. Crawford, and E. P. Ivanova, ACS Nano **9**, 8458 (2015).
[108]W. Liu, X. Liu, J. Fangteng, S. Wang, L. Fang, H. Shen, S. Xiang, H. Sun, and B. Yang, Nanoscale **6**, 13845 (2014).
[109]S. Wu, Y. Huang, T. Hsueh, and C. Liu, Jpn. J. Appl. Phys. **47**, 4906 (2008).
[110]P. K. Yadav, P. Lemoine, G. Dale, J. W. J. Hamilton, P. S. M. Dunlop, J. A. Byrne, P. Mailley, and C. Boxall, Appl. Phys. A: Mater. Sci. Process. **119**, 107 (2015).